J|A|C|S
ARTICLES
Published on Web 12/19/2007

Rapid Protein−Ligand Costructures Using Chemical Shift Perturbations

Jaime Stark and Robert Powers*

Department of Chemistry, University of Nebraska-Lincoln, Lincoln, Nebraska 68588

Received May 25, 2007; E-mail: rpowers3@unl.edu

Abstract: Structure-based drug discovery requires the iterative determination of protein−ligand costructures in order to improve the binding affinity and selectivity of potential drug candidates. In general, X-ray and NMR structure determination methods are time consuming and are typically the limiting factor in the drug discovery process. The application of molecular docking simulations to filter and evaluate drug candidates has become a common method to improve the throughput and efficiency of structure-based drug design. Unfortunately, molecular docking methods suffer from common problems that include ambiguous ligand conformers or failure to predict the correct docked structure. A rapid approach to determine accurate protein−ligand costructures is described based on NMR chemical shift perturbation (CSP) data routinely obtained using 2D $^{1}H-^{15}N$ HSQC spectra in high-throughput ligand affinity screens. The CSP data is used to both guide and filter AutoDock calculations using our AutoDockFilter program. This method is demonstrated for 19 distinct protein−ligand complexes where the docked conformers exhibited an average rmsd of 1.17 ± 0.74 Å relative to the original X-ray structures for the protein−ligand complexes.

Introduction

Structure-based drug design utilizes the known three-dimensional structures of biologically relevant proteins to develop drug candidates in a rational yet relatively rapid manner.[1,2] However, this process requires an in-depth understanding of the molecular processes that govern the interaction between a target protein and a potential drug. Knowledge of the precise location and orientation, or pose, of the drug molecule when bound to the protein−ligand complex can be experimentally determined using X-ray crystallography or NMR, but these techniques require a significant amount of time, usually on the order of weeks to months.[3,4] A number of NMR approaches have been described to shorten this time frame that includes NOE based protein−ligand models,[5,6] differential chemical shift perturbations between two or more bound ligands,[7] SOS-NMR,[8] and NMR-DOC.[9] These approaches still suffer from significant experimental drawbacks that limit their practical use to routine determination of a large number of protein−ligand costructures. In order to facilitate the high-throughput screening of thousands of compounds, the application of molecular docking simulations for filtering and evaluating drug candidates is a common alternative.[10]

Molecular docking is the process of predicting the structure of a protein−ligand complex using only the structures of the

Table 1. Rmsd Comparison between the Ligand-Bound and Unbound Proteins

PDB ID bound/unbound	rmsd (Å) full protein backbone[a]	rmsd (Å) binding site backbone[b]	rmsd (Å) binding site all atom[c]	resolution (Å)	refs
1A6W/1A6U	0.33	0.29	0.77	2.00/2.10	none
1ACJ/1QIF	0.38	0.30	0.63	2.80/2.10	44/45
1BLH/1DJB	0.25	0.20	1.39	2.30/2.10	46/47
1BYB/1BYA	0.29	2.48	2.36	1.90/2.20	48/48
1C83/1SUG	0.23	0.19	0.77	1.83/1.95	49/50
1IVD/1NNA	1.04	0.54	0.82	1.90/2.50	51/52
1LPC/1LP8	0.14	0.27	0.58	1.70/1.65	53/53
1MRG/1AHC	0.27	0.17	1.15	1.80/2.00	54/55
1MTW/2TGA	0.34	0.93	1.10	1.90/1.80	56/57
1QPE/3LCK	0.25	0.31	0.40	2.00/1.70	58/59
1RBP/1BRQ	0.59	0.73	1.55	2.00/2.50	60/61
1SNC/1STN	0.67	0.85	2.09	1.65/1.70	62/63
1STP/2RTA	0.77	0.40	1.11	2.60/1.39	64/65
2CTC/2CTB	0.17	0.38	1.72	1.40/1.50	66/66
2H4N/2CBA	0.21	0.17	0.26	1.90/1.54	67/68
2PK4/1KRN	0.50	0.25	1.10	2.25/1.67	69/70
2SIM/2SIL	0.14	0.16	0.23	1.60/1.60	71/71
3PTB/2PTN	0.11	0.16	0.31	1.70/1.55	72/57
6CPA/5CPA	0.36	0.52	1.68	2.00/1.54	73/74

[a] The N, C′, and Cα atoms for all the residues in the protein structure were used for the rmsd calculation. [b] The N, C′, and Cα atoms for all the residues in the ligand binding site were used for the rmsd calculation. Amino acid residues in the ligand binding site were identified by having at least one atom within 6 Å of any ligand atom. [c] All atoms for all residues in the ligand binding site were used for the rmsd calculation.

(1) Congreve, M.; Murray, C. W.; Blundell, T. L. *Drug Discovery Today* **2005**, *10*, 895−907.
(2) Orry, A. J. W.; Abagyan, R. A.; Cavasotto, C. N. *Drug Discovery Today* **2006**, *11*, 261−266.
(3) Scapin, G. *Curr. Pharm. Design* **2006**, *12*, 2087−2097.
(4) Powers, R. *J. Struct. Funct. Genomics* **2002**, *2*, 113−123.
(5) Moy, F. J.; Chanda, P. K.; Chen, J. M.; Cosmi, S.; Edris, W.; Skotnicki, J. S.; Wilhelm, J.; Powers, R. *Biochemistry* **1999**, *38*, 7085−7096.
(6) Chen, J. M.; Nelson, F. C.; Levin, J. I.; Mobilio, D.; Moy, F. J.; Nilakantan, R.; Zask, A.; Powers, R. *J. Am. Chem. Soc.* **2000**, *122*, 9648−9654.
(7) Medek, A.; Hajduk, P. J.; Mack, J.; Fesik, S. W. *J. Am. Chem. Soc.* **2000**, *122*, 1241−1242.
(8) Chen, A.; Shapiro, M. J. *J. Am. Chem. Soc.* **1998**, *120*, 10258−10259.
(9) Pellecchia, M.; Meininger, D.; Dong, Q.; Chang, E.; Jack, R.; Sem, D. S. *J. Biomol. NMR* **2002**, *22*, 165−173.
(10) Kitchen, D. B.; Decornez, H.; Furr, J. R.; Bajorath, J. *Nat. Rev. Drug Discovery* **2004**, *3*, 935−949.

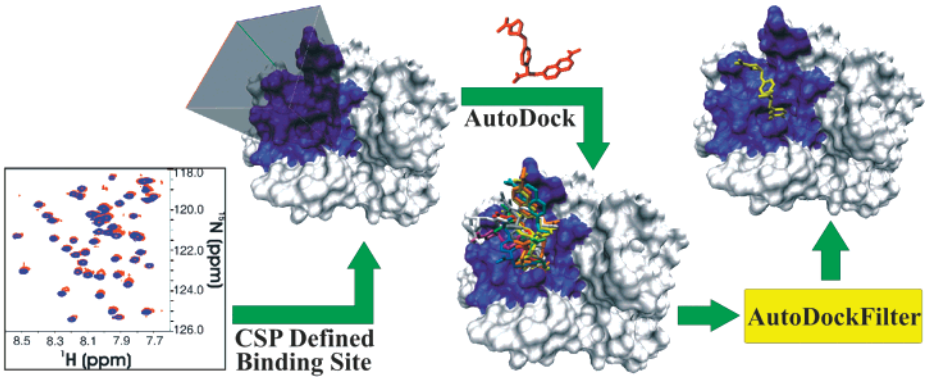

Figure 1. Flow diagram illustrating the overall process of generating a rapid protein−ligand costructure using CSP data to guide and filter the molecular docking results from AutoDock.

individual components. Most molecular docking software applications have two key parts: (1) a search algorithm that samples different locations and conformations of the ligand with respect to the protein and (2) a scoring method to evaluate the results of the search algorithm.[11] For molecular docking to be useful in drug discovery, these key parts should be both fast and accurate. These two requirements are often in opposition to each other, requiring necessary compromises that commonly end in ambiguous results or failure.[12−16] There are numerous molecular docking software applications that utilize different searching and scoring algorithms, where AutoDock is currently the most cited of these applications[17] and has been demonstrated to outperform other docking tools in a virtual screen of a compound library.[15]

In AutoDock 4,[18,19] the protein is represented as a three-dimensional grid which is searched with a Lamarckian genetic algorithm that explores the different translational, rotational, and torsional degrees of freedom of the ligand relative to the grid. An estimated free energy of binding is used to evaluate the docked ligand conformations and comprises several terms that include dispersion/repulsion, directional hydrogen bonding, electrostatics, desolvation, and conformational energy. As a result of the searching algorithm, the accuracy of an AutoDock calculation is often dependent on the number of torsional degrees of freedom in the ligand and the size of the grid that represents the protein or the binding site.[16,20] The accuracy can be improved by increasing both the population size and the number of energy evaluations for the Lamarckian genetic algorithm.[16,21] Unfortunately, these modifications often lead to a drastic increase in computational time (tens of hours) that significantly reduces the throughput required for iterative structure-based drug design. Furthermore, increasing these parameters does not guarantee that the lowest-energy conformer predicted by AutoDock will result in a correct protein−ligand model.

Prior knowledge of the ligand binding site would potentially improve the accuracy of the docking calculations by minimizing the grid volume that must be searched as well as limiting the possible conformations of the ligand that have energetically favorable interactions with the protein.[16] One rapid method of locating the binding site is by identifying the amino acid residues that experience chemical shift perturbations in a 2D ^{1}H−^{15}N HSQC NMR titration experiment due to their proximity to the bound ligand.[7,22,23]

Chemical shift perturbations (CSPs) can also be used to filter the docking results by selecting a pose consistent with the observed chemical shift changes.[24] The protein−protein docking program HADDOCK[25] uses CSPs and mutagenesis to create ambiguous interaction restraints, which define an upper boundary for the distance one residue may be from any atom of the bound molecule. These restraints are combined with a complete set of structural restraints that define the protein-free conformation in a simulated annealing protocol using CNS[26] to calculate a costructure. A similar approach can be used to provide criteria to select the best ligand conformation(s) generated from an AutoDock calculation.

Our approach for rapidly determining an accurate ligand binding orientation utilizes CSPs from a 2D ^{1}H−^{15}N HSQC NMR experiment to both guide and filter an AutoDock costructure calculation. By using CSPs to define the likely ligand binding site, the AutoDock 3D grid is reduced to a volume encompassing only the binding site, thus decreasing the search space traversed by the ligand. Furthermore, an NMR energy function based on the magnitude of CSPs is shown to be an effective filtering tool to select the best ligand conformation.

Experimental Section

Preparation of the Ligand and Target Protein. The analysis of the reliability of using CSPs to guide and filter molecular docking was demonstrated with the X-ray structures for 19 distinct protein−ligand

(11) Halperin, I.; Ma, B.; Wolfson, H.; Nussinov, R. *Proteins* **2002**, *47*, 409−443.
(12) Verkhivker, G. M.; Bouzida, D.; Gehlhaar, D. K.; Rejto, P. A.; Arthurs, S.; Colson, A. B.; Freer, S. T.; Larson, V.; Luty, B. A.; Marrone, T.; Rose, P. W. *J. Comput.-Aided Mol. Des.* **2000**, *14*, 731−751.
(13) Watson, J. D.; Laskowski, R. A.; Thornton, J. M. *Curr. Opin. Struct. Biol.* **2005**, *15*, 275−284.
(14) Arakaki, A. K.; Zhang, Y.; Skolnick, J. *Bioinformatics* **2004**, *20*, 1087−1096.
(15) Park, H.; Lee, J.; Lee, S. *Proteins* **2006**, *65*, 549−554.
(16) Hetenyi, C.; Van Der Spoel, D. *Protein Sci.* **2002**, *11*, 1729−1737.
(17) Sousa, S. F.; Fernandes, P. A.; Ramos, M. J. *Proteins* **2006**, *65*, 15−26.
(18) Morris, G. M.; Goodsell, D. S.; Halliday, R. S.; Huey, R.; Hart, W. E.; Belew, R. K.; Olson, A. J. *J. Comput. Chem.* **1998**, *19*, 1639−1662.
(19) Huey, R.; Morris, G. M.; Olson, A. J.; Goodsell, D. S. *J. Comput. Chem.* **2007**, *28*, 1145−1152.
(20) Bursulaya, B. D.; Totrov, M.; Abagyan, R.; Brooks, C. L., III. *J. Comput. Aided Mol. Des.* **2003**, *17*, 755−763.
(21) Hetenyi, C.; van der Spoel, D. *FEBS Lett.* **2006**, *580*, 1447−1450.
(22) Shuker, S. B.; Hajduk, P. J.; Meadows, R. P.; Fesik, S. W. *Science* **1996**, *274*, 1531−1534.
(23) McCoy, M. A.; Wyss, D. F. *J. Am. Chem. Soc.* **2002**, *124*, 11758−11763.
(24) Schieborr, U.; Vogtherr, M.; Elshorst, B.; Betz, M.; Grimme, S.; Pescatore, B.; Langer, T.; Saxena, K.; Schwalbe, H. *ChemBioChem* **2005**, *6*, 1891−1898.
(25) Dominguez, C.; Boelens, R.; Bonvin, A. M. J. J. *J. Am. Chem. Soc.* **2003**, *125*, 1731−1737.
(26) Brunger, A. T.; Adams, P. D.; Clore, G. M.; DeLano, W. L.; Gros, P.; Grosse-Kunstleve, R. W.; Jiang, J.-S.; Kuszewski, J.; Nilges, M.; Pannu, N. S.; Read, R. J.; Rice, L. M.; Simonson, T.; Warren, G. L. *Acta Crystallogr., Sect. D* **1998**, *D54*, 905−921.

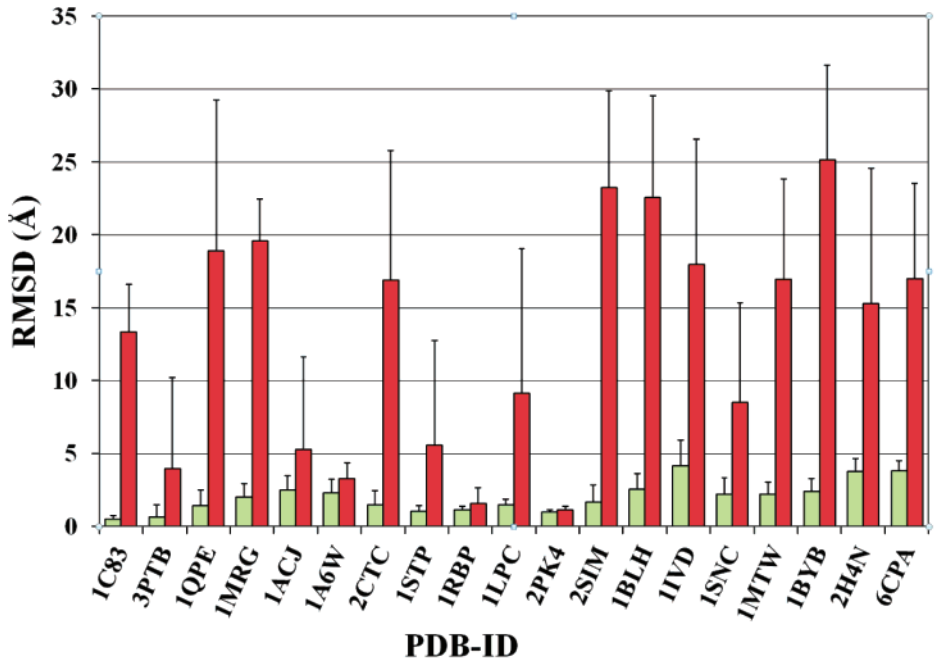

Figure 2. Comparison of rmsd values of the docked ligand conformers relative to the original ligand conformation in the protein−ligand X-ray structure. AutoDock calculations used either CSP-guided docking without ADF filtering (green) or blind docking (red). Conformers within 2.2 kcal/mol of the lowest-energy conformer were selected.

complexes (Table 1) present in the Protein Data Bank (http://www.pdb.org).[27,28] The ligands were removed from the protein−ligand complex and saved as a separate coordinate file. All solvent molecules and ions were also removed with the exception of ions deemed to be biologically relevant to ligand binding. Any missing heavy atoms for the amino acid residues were added using Swiss-PDBViewer (http://www.expasy.org/spdbv).[29] All hydrogens were added to the protein and ligand using standard protonation states at a neutral pH.

Docking was also performed using the corresponding unbound structures for each of the 19 protein−ligand complexes. This permitted a comparison of the docking performance using both bound and unbound protein structures. Protein files were prepared in the same manner as above. In addition, the backbone coordinates of the apoprotein were aligned with the bound protein structure prior to the AutoDock calculation (Table 1). The ligand conformation in the original X-ray structure of the complex was then used to measure a root mean square deviation (rmsd) between the docked ligand conformers calculated using the bound and apoprotein structures.

Prediction of Ligand Binding Sites and Chemical Shift Perturbations. The NMR-predicted binding site for each protein complex was determined by identifying all of the amino acid residues within 6.0 Å of any atom in the ligand using RasMol 2.7.3.1.[30] These are the residues that are anticipated to incur a chemical shift perturbation when the protein is titrated with the ligand. The coordinates of the residues that compose this binding site were then saved as a separate structure file that was used to define the grid size for the guided docking. Chemical shift perturbations were then estimated using a simple linear relationship based on the distance between the amide nitrogen for each residue in the binding site to the nearest ligand atom.

Molecular Docking. AutoDock 4.01[18,19] with the AutoDockTools 1.4.5 (http://mgltools.scripps.edu) graphical interface was used to simulate 120 different binding conformations for each protein−ligand pair. In the analysis where the docking was not guided by the NMR-predicted binding site (blind docking), grid maps were generated with 0.547 Å spacing and set to an appropriate size that encompasses the entire protein. The CSP-guided docking analysis also used the 0.547 Å spacing, but the grid map size was set to encompass those amino acid residues that were determined to be within 6.0 Å of the ligand. The docking calculations were performed using the Lamarckian genetic algorithm default settings with a population size of 300 and 500,000 energy evaluations. The AutoDock calculations took, on average, 37 ± 32 min per protein−ligand pair to complete on an Intel Xeon 3.06 GHz dual processor Linux workstation. The calculation time increased proportionally with the number of rotatable bonds in the ligand.

Filtering of Docked Ligand Conformations. The resulting 120 docked ligand conformations were filtered using our AutoDockFilter (ADF) program, which utilizes the magnitude of the chemical shift perturbations to select the best conformers instead of relying on the ambiguity inherent in choosing the best cluster based solely on the AutoDock empirical binding energy.

ADF calculates a pseudodistance (d_{CSP}) based on the magnitude of the NH chemical shift perturbations for each residue in a $^{1}H-^{15}N$ HSQC NMR experiment. We are assuming linear relationships between the magnitudes of the CSPs and the distances to the nearest ligand atom. Also, the shortest possible CSP pseudodistance allowed is 3 Å. This minimizes any bias to large chemical shift changes that may result from multiple factors in addition to proximity of the ligand. This pseudodistance is then compared to the shortest distance (d_s) between any atom in the residue that incurred an NH CSP and any atom in each docked ligand conformer. A violation energy is attributed to the conformer only when the shortest distance in the docked protein−ligand costructure is larger than the pseudodistance predicted from CSPs. Thus, the pseudodistance based on CSP only represents an upper distance boundary. The violation energy is summed for each separate CSP to generate an overall NMR energy (E_{NMR}).

$$E_{NMR} = k \sum_{i=1}^{n} (\Delta_{Dist})^2$$

where

(27) Berman, H.; Henrick, K.; Nakamura, H. *Nat. Struct. Biol.* **2003**, *10*, 980.
(28) Berman, H. M.; Westbrook, J.; Feng, Z.; Gilliland, G.; Bhat, T. N.; Weissig, H.; Shindyalov, I. N.; Bourne, P. E. *Nucleic Acids Res.* **2000**, *28*, 235−242.
(29) Guex, N.; Peitsch, M. C. *Electrophoresis* **1997**, *18*, 2714−23.
(30) Sayle, R. A.; Milner-White, E. J. *Trends Biochem. Sci.* **1995**, *20*, 374.

$$\Delta_{\text{Dist}} = \begin{cases} d_{\text{CSP}} - d_s & d_{\text{CSP}} < d_s \\ 0 & d_s \leq d_{\text{CSP}} \end{cases} \quad (1)$$

An rmsd is then calculated by ADF between each docked ligand conformation relative to the ligand with the lowest NMR energy. The structures are then clustered based on this rmsd value using the *k*-means method.[31] If a particular docked conformation has an NMR energy that is beyond two standard deviations from the average, it is excluded from the cluster. Only the best cluster from ADF is used for further analysis. The graphical representations of the proteins and ligands in this paper were prepared using VMD Molecular Graphics Viewer.[32]

Molecular Docking Using a Flexible Binding Site. A new feature in AutoDock 4.01 allows for rotatable bonds in the side chain of any selected residue in the receptor protein. A flexible binding site was used in the docking of tacrine to the free acetylcholinesterase structure (PDB-ID: 1QIF). This was done to account for the observation that Phe 330 had flipped into the active site of acetylcholinesterase, partially blocking access to tacrine. Seven residues within the previously defined binding site were allowed to have flexible sidechains: Trp84, Tyr121, Phe330, Tyr334, Trp432, His440, and Tyr442. The amino acids were chosen based on their proximity to Phe330 and tacrine in the X-ray crystal structure of the complex (PDB-ID: 1ACJ). Not all of the residues in the binding site were defined as a flexible due to a limitation in the number of allowable rotatable bonds. The AutoDock calculation with flexible side chains took approximately 4.5 h to complete using the identical docking parameters and computer hardware as the previous calculations.

Molecular Docking Using Experimental NMR Data. A further analysis of CSPs to guide and filter an AutoDock molecular docking calculation was performed using published ^{1}H and ^{15}N chemical shift data obtained from the solution structure of staphylococcal nuclease in both the unbound[33] and thymidine 3′,5′-bisphosphate complexed forms.[34,35] The magnitudes of the CSPs were calculated using a common weighting approach:

$$\text{CSP} = \sqrt{\frac{\left(\frac{\delta_N}{5}\right)^2 + \delta_H{}^2}{2}} \quad (2)$$

where δ_N and δ_H represent respectively the changes in ^{15}N and ^{1}H chemical shifts upon ligand binding.[36]

The binding site was determined by first selecting residues with CSPs greater than one standard deviation from the mean and mapping these residues onto the *Staphylococcus aureus* molecular surface. These residues corresponded to Ile18, Asp19, Phe34, Leu37, Leu38, Val39, Lys84, Ala60, Lys110, Tyr113, Val114, and Tyr115. This was further filtered by visually selecting only those residues that clustered together on the protein's molecular surface, consistent with a consensus binding site. It is important to select the residues predicted to interact with the ligand in the consensus binding site. Some general factors that were considered include the presence of a contiguous surface of residues with CSPs (residues separated by <5 Å from nearest neighbors), residues clustered about a central point (encircling a binding pocket), surface accessibility, proximity to a surface feature (presence of intervening residues), relative distance to the main cluster of residues, and the relative magnitude of the observed CSPs. Another consideration is the number of residues that form a cluster, where a larger cluster size (≥4) increases the likelihood that a ligand binding site has been correctly identified.

Residues Leu37, Leu38, Val39, Tyr113, Val114, and Tyr115 form the main contiguous CSP surface along one edge of a pocket on the *S. aureus* molecular surface. Residues Ile18, Asp19, and Lys84 exhibit some of the largest CSPs and are proximal to the same pocket as the main CSP cluster of six residues. In effect, residues Ile18, Asp19, Leu37, Leu38, Val39, Lys84, Tyr113, Val114, and Tyr115 encircle this binding pocket. Residue Ala60 was excluded because it is >10 Å from this main cluster of residues and is on the opposite face of the protein. Residue Phe34 was excluded because it is not surface exposed and is part of the hydrophobic core of the protein. Residue Lys110 was excluded because it is outside the ring of residues encircling the binding pocket (i.e., residues Val39 and Tyr 113 separate Lys110 from the binding pocket). Lys 110 would not be expected to interact directly with thymidine 3′,5′-bisphosphate. It also had the second-lowest CSP among the 12 residues initially selected.

Docking calculations were performed using the X-ray structures of the unbound (PDB-ID: 1EY0) and the thymidine 3′,5′-bisphosphate complexed (PDB-ID: 1SNC) staphylococcal nuclease protein structure. The ligand coordinates were removed from the protein−ligand complex and stored as a separate file for docking. The AutoDock grid was positioned and sized to cover the residues with experimental CSPs. The grid was also large enough to include the entire thymidine 3′,5′-bisphosphate molecule. Docking calculations were performed using the same parameters as before. Filtering of results using ADF was performed using the experimental CSPs.

Results and Discussion

The overall methodology for the rapid determination of a protein−ligand costructure has three steps (Figure 1): (i) identification of the binding site by mapping CSPs from a ^{1}H−^{15}N HSQC NMR experiment, (ii) guiding the AutoDock calculations using the identified binding site, and (iii) using the relative magnitude of the CSPs to filter the resulting ligand conformers from AutoDock. The ability of the protocol to accurately predict a protein−ligand costructure based on CSPs was demonstrated using multiple model systems and an experimental data set for *S. aureus* nuclease complexed to thymidine 3′,5′-bisphosphate.

Protein−Ligand Model Systems. Due to the scarcity of available chemical shift and structural data for complexed and unbound forms of multiple protein−ligand systems, the methodology was primarily demonstrated using empirically predicted chemical shift perturbations based on existing X-ray structures in the PDB. A total of 19 distinct pairs of protein structures with a variety of biological activity were identified and used for the docking simulation (Table 1).

NMR chemical shift changes are routinely and widely used to map protein−ligand interactions based on the generally accepted protocol that residues proximal to the bound ligand will experience higher CSPs compared to residues distal to the ligand binding site.[38,39] Thus, CSPs were estimated by assuming a simple linear relationship between the magnitude of the CSPs and the distance from the amino acids' NH atoms and the nearest ligand atom. This is

(31) Kanungo, T.; Mount, D.; Netanyahu, N.; Piatko, C.; Silverman, R.; Wu, A. A Local Search Approximation Algorithm for *k*-Means Clustering. In *Proceedings of the 18th Annual Symposium on Computational Geometry*, Barcelona, Spain, 2002; ACM: New York, 2002; pp 10−18.
(32) Humphrey, W.; Dalke, A.; Schulten, K. *J. Mol. Graph* **1996**, *14*, 33−38, 27−28.
(33) Wang, J. F.; Hinck, A. P.; Loh, S. N.; LeMaster, D. M.; Markley, J. L. *Biochemistry* **1992**, *31*, 921−36.
(34) Wang, J. F.; Hinck, A. P.; Loh, S. N.; Markley, J. L. *Biochemistry* **1990**, *29*, 102−113.
(35) Wang, J. F.; LeMaster, D. M.; Markley, J. L. *Biochemistry* **1990**, *29*, 88−101.
(36) Garrett, D. S.; Seok, Y. J.; Peterkofsky, A.; Clore, G. M.; Gronenborn, A. M. *Biochemistry* **1997**, *36*, 4393−4398.
(37) Wang, J.; Truckses, D. M.; Abildgaard, F.; Dzakula, Z.; Zolnai, Z.; Markley, J. L. *J. Biomol. NMR* **1997**, *10*, 143−164.
(38) Carlomagno, T. *Annu. Rev. Biophys. Biomol. Struct.* **2005**, *34*, 245−266.
(39) Lepre, C. A.; Moore, J. M.; Peng, J. W. *Chem. Rev.* **2004**, *104*, 3641−376.

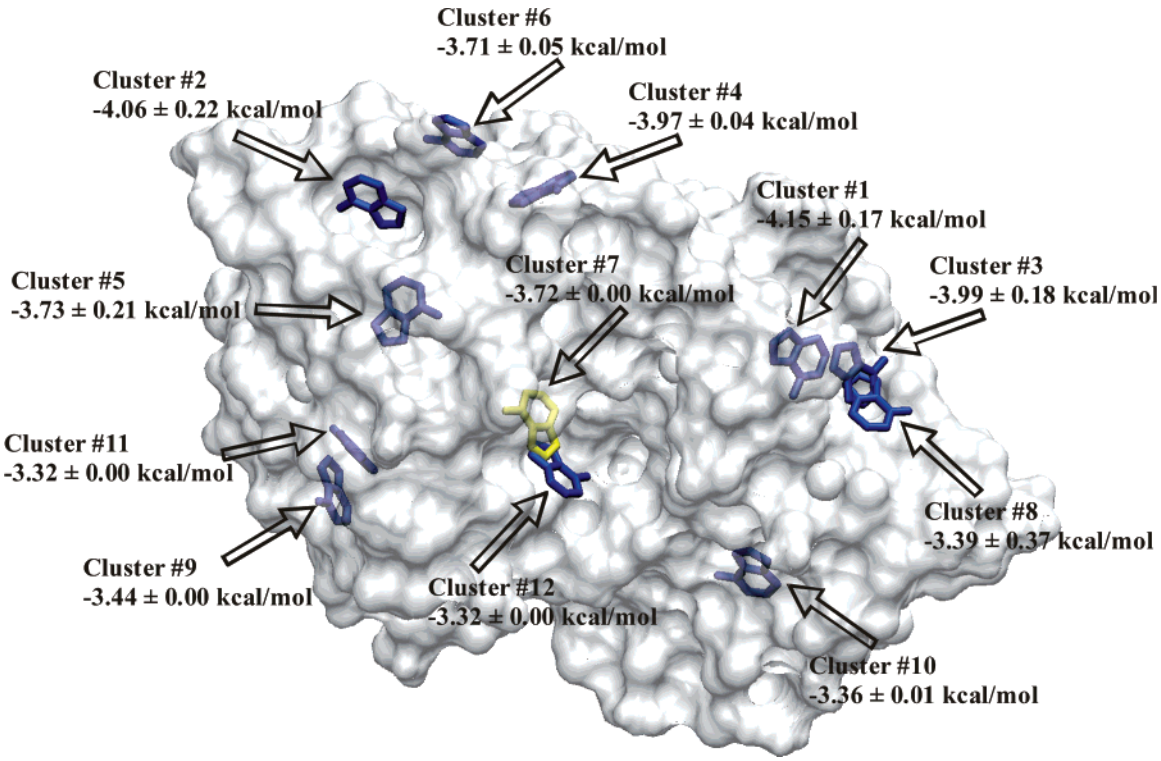

Figure 3. Surface representation of the ribosome-inactivating protein (PDB-ID: 1MRG) with the lowest-energy adenosine conformer for each cluster calculated by AutoDock superimposed on the protein structure. The conformer with the lowest rmsd relative to the X-ray structure is colored yellow. Each cluster is labeled with the cluster ranking, the average binding energies, and standard deviation of the binding energies.

clearly a simple approximation since other factors besides proximity to the bound ligand contribute to CSPs. These factors include hydrogen bonding, electrostatics and ring current effects.[40] Unfortunately, a robust approach to predict ligand-induced chemical shift changes in a protein−ligand system using ab initio methods is not available because of the complexity of the system (e.g., number of atoms).

The absolute magnitude of the predicted CSPs is not critical since the CSPs are only used as an upper bound constraint to filter the poses predicted by AutoDock. Additionally, a 3 Å distance cutoff is used to avoid any bias or distortion from unusually large CSPs. Effectively, the relative magnitude of the CSPs determines the conformer(s) selected by our AutoDock-Filter (ADF) program. Again, this is based on the generally accepted premise that residues that incur that largest relative CSP are predicted to be closer to the docked ligand. ADF simply identifies the conformer that maximizes an interaction with residues with the largest CSPs. This is also similar to the protocol implemented by HADDOCK[25] where CSPs and mutagenesis are used to create ambiguous interaction restraints, which define upper boundaries for the distances residues may be from any atom of the bound molecule in a protein−protein docking calculation.

Comparison of Blind Docking and CSP-Guided Docking. Blind docking is commonly used to generate protein−ligand complexes when a binding site is undetermined.[16,21] The approach requires scanning the entire protein surface, where the scoring function is used to both identify the binding site and select the best conformer. It may be extremely challenging to identify the correct ligand binding site when the binding energies between multiple distinct binding sites are within the error of the calculations. The AutoDock binding energies are estimated to have an error of 2.2 kcal/mol.[41] A comparison of results obtained between CSP-guided docking and blind docking demonstrates the expected advantages of guided docking to a known ligand binding site. On average, blind docking generated 63 ± 37 distinct clusters in AutoDock using a 2.0 Å rmsd tolerance for each cluster. This large number of clusters generated a corresponding large average rmsd of 15.40 ± 6.40 Å relative to the original X-ray structure.

The CSP-guided docking calculations yielded a relatively tight clustering of conformers (16 ± 23 distinct clusters) where the average rmsd was 2.31 ± 1.15 Å. This is a dramatic and expected improvement relative to blind docking. A comparison using all the conformers within 2.2 kcal/mol of the lowest-energy conformer was made between the CSP-guided and blind dockings. This comparison demonstrates that the average rmsd of the CSP-guided conformers was significantly better relative to the blind docking conformers (Figure 2). In addition, molecular dockings for ligands with greater than five rotatable bonds typically showed better results with the CSP-guided docking. Flexible ligands add a significant amount of complexity to the AutoDock calculation that is simplified by applying a smaller search space.

Focusing a docking calculation into a smaller volume of the protein minimizes the search space for the ligand and allows the docking resources to be spent orienting the ligand into an energetically favorable position and conformation instead of finding the binding site. Using the binding site determined by CSPs to focus an AutoDock grid is expected to eliminate some of the inherent ambiguity in identifying the correct ligand pose

(40) Oldfield, E. *Annu. Rev. Phys. Chem.* **2002**, *53*, 349−378.

(41) Rosenfeld, R. J.; Goodsell, D. S.; Musah, R. A.; Morris, G. M.; Goodin, D. B.; Olson, A. J. *J. Comput. Aided Mol. Des.* **2003**, *17*, 525−536.

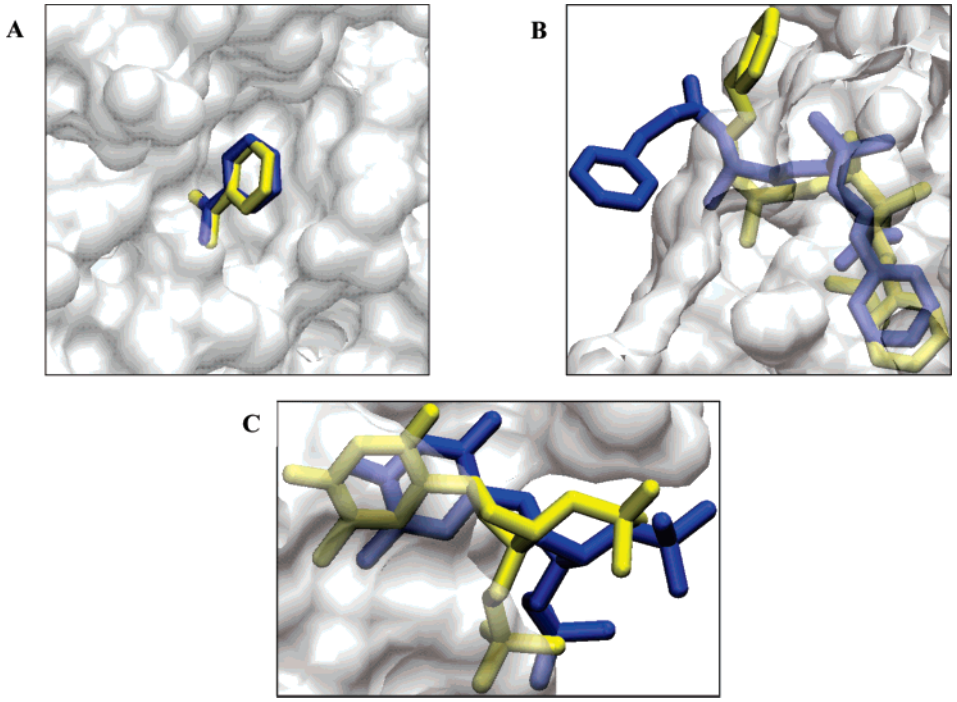

Figure 4. Superposition of the CSP-guided docking with ADF filtering conformers (blue) with the original X-ray structures (yellow) for (A) benzamidine complexed with trypsin (PDB-ID: 3PTB), (B) a phosphonate complexed with carboxypeptidase (PDB-ID: 6CPA), and (C) *S. aureus* nuclease complexed to thymidine 3′,5′-bisphosphate (PDB-ID: 1SNC). The nuclease-thymidine 3′,5′-bisphosphate docked model is based on experimental NMR chemical shift data.

since the uncertainty regarding the correct ligand binding site has been removed.

Lowest-Energy Cluster is Not Necessarily the Best Conformer. Using a blind approach, AutoDock calculates a large number of clusters that are clearly outside of the known ligand binding site observed in the original X-ray crystal structure (Figure 3). For AutoDock, selecting the lowest-energy cluster and the most populated cluster are the two most common methods for identifying the most accurate conformers. In our analysis, the lowest-energy cluster represented the best docked conformers in 10 out of the 19 docking calculations performed (53% accuracy). The best docked cluster of conformers was only selected in 6 instances (32% accuracy) when the most populated cluster was used, and 5 of those were also the lowest-energy cluster. This causes a significant ambiguity in evaluating the accuracy of any particular protein−ligand costructure based solely on the AutoDock binding energy. However, it should be noted that AutoDock does generate at least one conformer out of the 120 conformers that is within 2.0 Å of the actual binding pose in 14 out of the 19 protein−ligand blind docking calculations. Thus, an accurate conformer is often generated by an AutoDock calculation, but the binding energy is not a reliable mechanism to identify the best conformer.

One of the main reasons the lowest-energy cluster may not contain the most accurately docked conformer appears to arise from the low sensitivity of the AutoDock binding energy to identify distinct binding sites and ligand conformations. This is especially true when the relative differences in the binding energies between the clusters calculated by AutoDock are taken into consideration. A representative conformer for each cluster calculated by AutoDock for adenosine docked to the ribosome-inactivating protein (RIP, PDB-ID: 1MRG) is illustrated in Figure 3. A difference of only 0.83 kcal/mol is observed between the lowest- and highest-energy clusters. This energy difference is significantly smaller than the 2.2 kcal/mol estimate for the error in the AutoDock binding energy. Thus, the lowest-energy cluster is not appreciably different from the remaining clusters in the docking of adenosine to RIP. Specifically, an energy difference of only 0.43 kcal/mol is observed between the cluster with the lowest rmsd relative to those of the X-ray structure and the lowest-energy cluster. If the error in the AutoDock binding energy follows a normal distribution, this would partially explain why the correct conformer is not always present in the lowest-energy cluster.

An additional reason the best conformer is not present in the lowest-energy cluster may be attributed to the protocol AutoDock uses to define members of a cluster. AutoDock selects the conformer with the lowest binding energy to represent the first conformer of the first cluster. Conformers that are within the rmsd tolerance of the lowest-energy conformer (2.00 Å for this study) are placed in the first cluster regardless of binding energy. The remaining conformer with the lowest binding energy starts the next cluster that will include all of the remaining conformers within the rmsd tolerance. This continues until all of the conformers are placed in a cluster. Thus, the best conformer can easily be excluded from the first cluster, despite similar binding energies.

Even though the conformers in any particular cluster are within 2.0 Å of each other, the binding energies can vary enough that some conformers in the lowest-energy cluster actually have a higher binding energy than conformers in other clusters. This again suggests that simply using the binding energy to select for the best pose is ambiguous and unreliable for any specific protein−ligand costructure.

On the basis of our results, choosing the lowest-energy cluster in a blind docking will result in identifying an incorrect binding

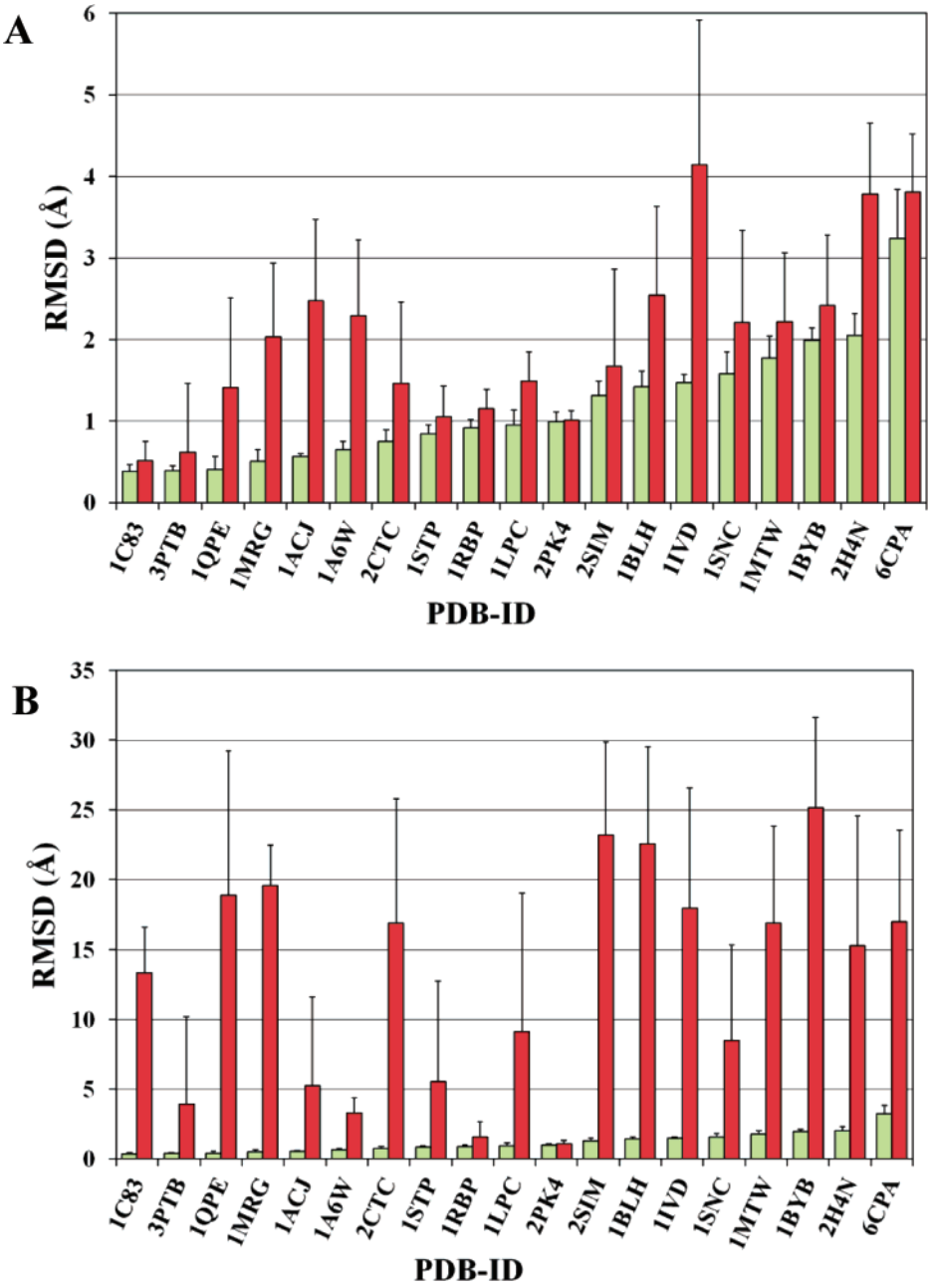

Figure 5. Comparison of rmsd values of the docked ligand conformers relative to the original ligand conformation in the protein−ligand X-ray structure. AutoDock calculations used the CSP-guided docking with ADF filtering (green) and (a) the CSP-guided docking without ADF filtering (red) or (b) blind docking (red). Conformers within 2.2 kcal/mol of the lowest-energy conformer were selected for the CSP-guided docking without ADF filtering and blind docking.

site and a wrong conformer 47% of the time. Interestingly, the lowest-energy cluster represents the best docked pose in 14 of the 19 docking calculations with CSP-guided docking. Again, this is a significant improvement relative to blind docking; however, an ambiguity in identifying the correct conformer still remains. A wrong conformer is still identified 26% of the time. This ambiguity can be remedied by also using the CSPs to further filter the docking results to select conformers that agree with the NMR experimental data.

CSP-Guided Docking with ADF filtering. Our AutoDock-Filter (ADF) program identifies the "best" conformer from an AutoDock calculation based on a consistency with the experimental CSPs. ADF replaces the ambiguous AutoDock binding energy with an NMR violation energy (eq 1). The ADF-selected conformer has a minimal distance between each protein residue with a CSP and the docked ligand. Filtering the CSP-guided docking with ADF consistently resulted in the identification of a cluster of conformers with a high similarity to the original X-ray costructure (Figure 4A). This is a significant improvement in accuracy relative to the blind docking and the CSP-guided docking without ADF. It completely eliminates the ambiguity encountered by relying on the AutoDock binding energy.

Obtaining an rmsd <3 Å from an experimental protein−ligand structure is generally considered a good result in a docking calculation.[42] The conformers selected from the CSP-guided docking with ADF filtering had rmsd averages of 1.17

(42) Wolf, A.; Zimmermann, M.; Hofmann-Apitius, M. *J. Chem. Inf. Model* **2007**, *47*, 1036−1044.

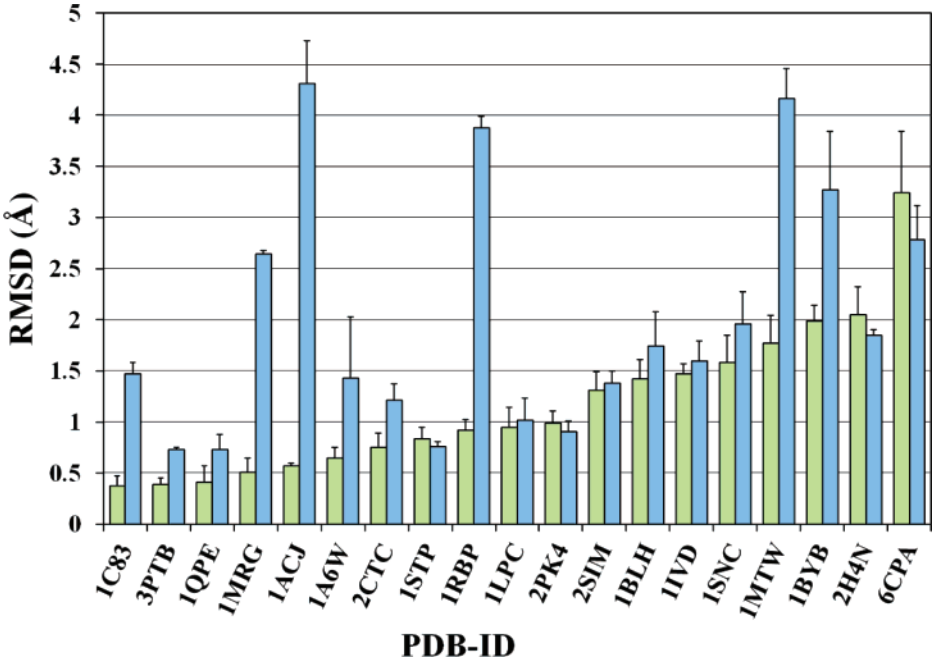

Figure 6. Comparison of rmsd values of the best docked ligand conformers relative to the original ligand conformation in the protein−ligand X-ray structure. The AutoDock calculation was performed by docking the ligand to either the bound protein structure (green) or the free protein structure (blue). The calculations used CSP-guided docking followed by ADF filtering to select the best conformers.

± 0.74 Å. These results are also significantly better than the conformers selected by CSP-guided docking without ADF filtering (2.02 ± 1.05 Å). The improvement is even more pronounced when compared to blind docking (12.91 ± 7.81 Å). Figure 5 illustrates the improvement obtained using the CSP-guided docking with ADF filtering for each of the 19 protein−ligand structures. Thus, the CSP-guided docking with ADF filtering represents a significant improvement in rapidly obtaining accurate protein−ligand structures.

Only one ligand docking exhibited an average rmsd of over 2.00 Å when guided and filtered using CSPs. The relatively large rmsd average and deviation for phosphonate docked to carboxypeptidase A (PDB-ID: 6CPA) occurs because the ligand is partially solvent exposed (Figure 4B). In solution, this solvent-exposed region of the phosphonate is probably ill-defined and adopts multiple conformations similar to the results seen with AutoDock. Therefore, the higher rmsd difference observed between the X-ray structure and the docked conformer is irrelevant since the X-ray structure simply represents one of many equivalent conformations.

CSP-Guided Docking with ADF Filtering Using Apoproteins. A ligand binding to a protein structure may result in significant changes in the protein structure. This is illustrated by the backbone or active-site rmsd differences observed between the 19 apoprotein structures and the corresponding protein−ligand complexes (Table 1). A deviation as large as 2.48 Å is observed for the ligand binding site of β-amylase (PDB-ID: 1BYB, 1BYA) when it binds glucose. Therefore, the accuracy of the conformers obtained using the CSP-guided docking with ADF filtering protocol was further evaluated using unbound structures.

The AutoDock calculation and analysis was repeated using the 19 apoprotein structures following the identical procedure applied to the bound protein structures. The CSP-guided docking and ADF filtering with the apoproteins yielded results similar to those from the docking with the bound protein structures (Figure 6). However, there are four examples where docking of the ligand to the unbound protein structure resulted in a ≥2.00 Å increase in the rmsd relative to the corresponding protein−ligand X-ray structure. The observed rmsd binding site differences between the bound and free protein structures does not solely explain these docking results (Table 1). In fact, the protein X-ray structures with the largest binding site changes upon ligand binding did not necessarily yield significantly different docking results.

The worst docking results were seen with the free acetylcholinesterase structure (PDB-ID: 1QIF) that incurred a modest all atom deviation of 0.63 Å in the tacrine binding site between the bound and free X-ray structures. The best AutoDock-calculated tacrine conformer using the free acetylcholinesterase structure had a 3.91 Å rmsd from the original acetylcholinesterase-tacrine X-ray structure (PDB-ID: 1ACJ). This compares poorly to an average rmsd of 0.51 Å obtained for the tacrine conformers docked to the bound form of acetylcholinesterase. This large deviation in the docked tacrine conformers is due to the side chain of Phe 330 flipping into the free acetylcholinesterase binding site and essentially blocking tacrine from binding deep into the ligand pocket (Figure 7A). The side-chain flipping of Phe 330 is a known "gate keeper" mechanism of ligand binding to acetylcholinesterase.[43] This steric hindrance due to

(43) Kryger, G.; Silman, I.; Sussman, J. L. *Structure* **1999**, *7*, 297−307.
(44) Harel, M.; Schalk, I.; Ehret-Sabatier, L.; Bouet, F.; Goeldner, M.; Hirth, C.; Axelsen, P. H.; Silman, I.; Sussman, J. L. *Proc. Natl. Acad. Sci. U.S.A.* **1993**, *90*, 9031−9035.
(45) Weik, M.; Ravelli, R. B.; Kryger, G.; McSweeney, S.; Raves, M. L.; Harel, M.; Gros, P.; Silman, I.; Kroon, J.; Sussman, J. L. *Proc. Natl. Acad. Sci. U.S.A.* **2000**, *97*, 623−628.
(46) Chen, C. C.; Rahil, J.; Pratt, R. F.; Herzberg, O. *J. Mol. Biol.* **1993**, *234*, 165−178.
(47) Chen, C. C.; Smith, T. J.; Kapadia, G.; Wasch, S.; Zawadzke, L. E.; Coulson, A.; Herzberg, O. *Biochemistry* **1996**, *35*, 12251−12258.
(48) Mikami, B.; Degano, M.; Hehre, E. J.; Sacchettini, J. C. *Biochemistry* **1994**, *33*, 7779−7787.

side-chain dynamics appears to be a common source of docking error that was encountered using apoproteins.

Importantly, the magnitude of the NMR violation energy provides a valuable measure of the inherent accuracy of the AutoDock results and an efficient means to identify these incorrectly docked structures due to protein mobility. A comparison of the NMR violation energy with the rmsd between the docked and X-ray ligand structures is shown in Figure 8. An NMR violation energy >1500 is correlated with the poorly docked ligand conformers obtained with the apostructures. Therefore, obtaining a large NMR violation energy would call into question the reliability of the docked structure. This would imply that further analysis or a detailed dynamic simulation would be required in order to obtain an accurate docked protein−ligand costructure. Of course, the NMR violation threshold of 1500 is based on our simulated docking using empirically determined CSPs. This threshold may change for protein−ligand costructures that are calculated using experimentally determined CSPs.

Docking a ligand into a static protein structure is a common simplification to improve performance, but it is an assumption that can cause inaccuracies as observed above. AutoDock 4 attempts to alleviate the static receptor problem by incorporating side-chain flexibility in addition to the existing ligand flexibility. However, adding this additional flexibility significantly increases the AutoDock calculation time. Different ligand conformers now need to be evaluated against the various amino acid side-chain orientations in the binding site. AutoDock calculations using a static receptor required, on average, 37 ± 32 min. Conversely, an AutoDock calculation that docked tacrine into the free acetylcholinesterase structure allowing 7 amino acid side chains within the binding site to be flexible required 4.5 h to complete. Despite the dramatic increase in calculation time, there was a significant improvement in the accuracy of the docked tacrine structure (Figure 7B). The rmsd of the docked tacrine structure relative to the original X-ray structure dropped from 3.91 to 1.78 Å (Figure 8).

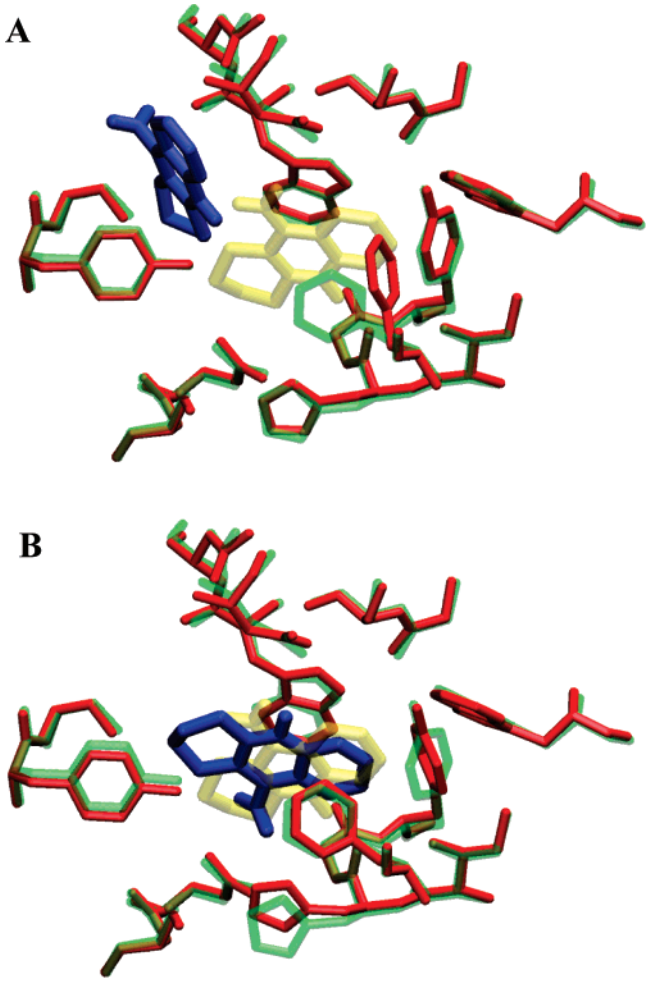

Figure 7. Comparison of tacrine docking to the free acetylcholinesterase structure (PDB-ID: 1QIF) using (A) static and (B) flexible acetylcholinesterase binding site residues. An overlay of the binding site residues (green) and tacrine (yellow) from the X-ray acetylcholinesterase-tacrine structure (PDB-ID: 1ACJ) with the binding site residues (red) for the free acetylcholinesterase structure used for the AutoDock calculation with the resulting best docked tacrine conformation (blue). The rmsd's between the docked and X-ray structure of tacrine using the static and flexible binding site are 3.91 and 1.78 Å, respectively.

Docking with Experimental NMR Data. While the analysis using empirically predicted chemical shift perturbations appears to support the reliability of using CSP-guided docking and ADF filtering to rapidly obtain accurate protein−ligand costructures, a full evaluation of the methodology requires an analysis with experimental chemical shift perturbation data. ^{1}H and ^{15}N chemical shift data for the free solution structure of staphylococcal nuclease[33] and the complex with thymidine 3′,5′-bisphosphate were readily available.[34,35] Similarly, the X-ray structures of the unbound (PDB-ID: 1EY0) and the complexed (PDB-ID: 1SNC) forms of staphylococcal nuclease were accessible through the PDB.

Experimental CSPs may arrive from either a direct interaction with the bound ligand or indirectly through a protein confor-

(49) Andersen, H. S.; Iversen, L. F.; Jeppesen, C. B.; Branner, S.; Norris, K.; Rasmussen, H. B.; Moller, K. B.; Moller, N. P. *J. Biol. Chem.* **2000**, *275*, 7101−7108.
(50) Pedersen, A. K.; Peters, G. G.; Moller, K. B.; Iversen, L. F.; Kastrup, J. S. *Acta Crystallogr., Sect. D* **2004**, *60*, 1527−1534.
(51) Jedrzejas, M. J.; Singh, S.; Brouillette, W. J.; Laver, W. G.; Air, G. M.; Luo, M. *Biochemistry* **1995**, *34*, 3144−3151.
(52) Bossart-Whitaker, P.; Carson, M.; Babu, Y. S.; Smith, C. D.; Laver, W. G.; Air, G. M. *J. Mol. Biol.* **1993**, *232*, 1069−1083.
(53) Kurinov, I. V.; Rajamohan, F.; Uckun, F. M. *Arzneim. Forsch.* **2004**, *54*, 692−702.
(54) Huang, Q.; Liu, S.; Tang, Y.; Jin, S.; Wang, Y. *Biochem. J.* **1995**, *309 (Pt. 1)*, 285−298.
(55) Ren, J.; Wang, Y.; Dong, Y.; Stuart, D. I. *Structure* **1994**, *2*, 7−16.
(56) Stubbs, M. T.; Huber, R.; Bode, W. *FEBS Lett.* **1995**, *375*, 103−107.
(57) Walter, J.; Steigemann, W.; Singh, T. P.; Bartunik, H.; Bode, W.; Huber, R. *Acta Crystallogr., Sect. B* **1982**, *38*, 1462−1472.
(58) Zhu, X.; Kim, J. L.; Newcomb, J. R.; Rose, P. E.; Stover, D. R.; Toledo, L. M.; Zhao, H.; Morgenstern, K. A. *Structure* **1999**, *7*, 651−661.
(59) Yamaguchi, H.; Hendrickson, W. A. *Nature* **1996**, *384*, 484−489.
(60) Cowan, S. W.; Newcomer, M. E.; Jones, T. A. *Proteins* **1990**, *8*, 44−61.
(61) Zanotti, G.; Ottonello, S.; Berni, R.; Monaco, H. L. *J. Mol. Biol.* **1993**, *230*, 613−624.
(62) Loll, P. J.; Lattman, E. E. *Proteins* **1989**, *5*, 183−201.
(63) Hynes, T. R.; Fox, R. O. *Proteins* **1991**, *10*, 92−105.
(64) Weber, P. C.; Ohlendorf, D. H.; Wendoloski, J. J.; Salemme, F. R. *Science* **1989**, *243*, 85−88.
(65) Katz, B. A. *J. Mol. Biol.* **1997**, *274*, 776−800.
(66) Teplyakov, A.; Wilson, K. S.; Orioli, P.; Mangani, S. *Acta Crystallogr., Sect. D* **1993**, *49*, 534−540.
(67) Lesburg, C. A.; Huang, C.; Christianson, D. W.; Fierke, C. A. *Biochemistry* **1997**, *36*, 15780−15791.
(68) Hakansson, K.; Carlsson, M.; Svensson, L. A.; Liljas, A. *J. Mol. Biol.* **1992**, *227*, 1192−11204.
(69) Wu, T. P.; Padmanabhan, K.; Tulinsky, A.; Mulichak, A. M. *Biochemistry* **1991**, *30*, 10589−10594.
(70) Stec, B.; Yamano, A.; Whitlow, M.; Teeter, M. M. *Acta Crystallogr., Sect. D* **1997**, *53*, 169−178.
(71) Crennell, S. J.; Garman, E. F.; Philippon, C.; Vasella, A.; Laver, W. G.; Vimr, E. R.; Taylor, G. L. *J. Mol. Biol.* **1996**, *259*, 264−280.
(72) Marquart, M.; Walter, J.; Deisenhofer, J.; Bode, W.; Huber, R. *Acta Crystallogr., Sect. B* **1983**, *39*, 480−490.
(73) Kim, H.; Lipscomb, W. N. *Biochemistry* **1990**, *29*, 5546−5555.
(74) Rees, D. C.; Lewis, M.; Lipscomb, W. N. *J. Mol. Biol.* **1983**, *168*, 367−387.

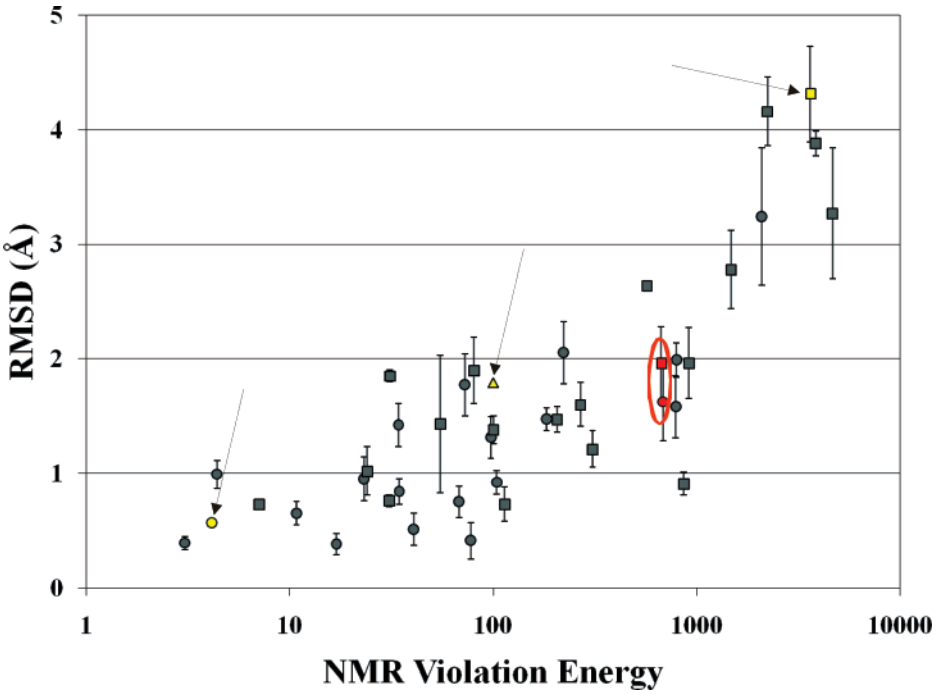

Figure 8. Comparison of the empirical NMR violation energy (logarithmic scale) against the corresponding rmsd for the best docked conformers using the bound form (●) and the free form (■) of the protein structure. The rmsd is relative to the ligand's conformation in the original X-ray structure. The circled data points correspond to the docking results using the experimental CSPs for staphylococcal nuclease. The docking results for acetylcholinesterase (PDB-ID: 1ACJ, 1QIF) are highlighted yellow and are indicated with an arrow. The acetylcholinesterase results also include the flexible protein docking results (seven residues) using the free protein structure (▲).

mational change that may occur distal from the ligand binding site. Thus, correct utilization of the CSPs to guide and filter an AutoDock calculation requires removing CSPs not resulting from a direct ligand interaction. In practice, CSPs greater than one standard deviation from the average CSP are mapped onto the protein surface to visually identify a consensus ligand binding site. This subset of CSPs is then used to guide the AutoDock grid for the docking calculation which is followed by ADF to select the best conformers based on consistency with these CSPs.

The experimental staphylococcal nuclease CSPs were used to guide and filter the docking of thymidine 3′,5′-bisphosphate to the bound conformation of the protein (Figure 4C). The best conformers using experimental CSPs had an average rmsd of 1.63 ± 0.35 Å relative to the original nuclease-thymidine 3′,5′-bisphosphate X-ray structure with a corresponding average NMR violation energy of 681 ± 333. These results compared well to the thymidine 3′,5′-bisphosphate conformers obtained with the empirical CSPs, where an average rmsd of 1.58 ± 0.27 Å and an average NMR violation energy of 788 ± 409 were obtained.

A similar comparison was observed for the docking of thymidine 3′,5′-bisphosphate to the unbound nuclease structure (PDB-ID: 1EY0). The experimental CSPs generated conformers with an average rmsd of 1.96 ± 0.32 Å and an average NMR violation energy of 667 ± 449 where the empirically predicted CSPs resulted in conformers with an average rmsd of 1.96 ± 0.31 Å and an average NMR violation energy of 914 ± 327. In effect, the experimental and empirical CSPs yielded essentially identical models of a nuclease-thymidine 3′,5′-bisphosphate costructure (Figure 8). This would suggest that the use of empirically predicted CSPs to evaluate the reliability of CSP-guided docking and ADF filtering method is a reasonable approach. Also, the results with the experimental staphylococcal nuclease data clearly indicate that the CSP-guided docking and ADF filtering method works equally well with experimental CSPs. It also suggests that an NMR violation threshold of 1500 may be applicable to identifying poorly docked structures using experimental CSPs since the NMR violation energies calculated for the nuclease-thymidine 3′,5′-bisphosphate costructure using experimental and empirical CSPs were similar. These results also demonstrate that the high accuracy obtained with the method is not simply an artifact of the empirical CSPs.

Conclusions

Combining experimental NMR chemical shift perturbations (CSPs) with AutoDock ligand docking calculations provides an efficient approach to rapidly obtain accurate (1.17 ± 0.74 Å) protein−ligand models. The CSPs are first used to guide an AutoDock calculation by defining the size and position of the AutoDock grid. The CSPs are then used in combination with our AutoDockFilter (ADF) program to select the best conformer cluster consistent with the CSPs using an empirical NMR violation energy. ADF assumes a linear relationship between the magnitude of CSPs and the distance between the ligand and the protein residues that incurred the CSP. The NMR violation energy correlates with the accuracy of the docked structures obtained using the empirical CSPs and the *S. aureus* nuclease experimental CSPs, where an observed energy >1500 implies an unreliably docked structure. The poor docking generally occurred with apoprotein structures that required a conformational change to accommodate the bound ligand. Additional protein dynamics such as side-chain flexibility are required to improve the accuracy of these docked ligands.

The docking method described in this paper typically requires 37 ± 32 min per protein−ligand complex. Since a 2D $^{1}H-^{15}N$ HSQC NMR experiment can be collected in ≤ 15 min, reliable and accurate protein−ligand costructures can be rapidly obtained in less than an hour. Thus, an efficient initial approach to structure-based drug discovery can be achieved by combining high-throughput NMR screening with CSP-guided and ADF-filtered AutoDock calculations. Of course, X-ray or NMR structures will still be required as the project matures since further refinement of the chemical leads mandates a higher-quality costructure than the 1−2 Å accuracy obtainable by molecular docking.

Acknowledgment. This work was supported by grants from the Nebraska Tobacco Settlement Biomedical Research Development Funds, the Nebraska Research Council, and the John C. and Nettie V. David Memorial Trust Fund. Research was performed in facilities renovated with support from the NIH under Grant RR015468-01.

JA0737974